Development/Plasticity/Repair

Developmental Spike Timing-Dependent Long-Term Depression Requires Astrocyte D-Serine at L2/3-L2/3 Synapses of the Mouse Somatosensory Cortex

Yuniesky Andrade-Talavera, Joaquín Sánchez-Gómez, Heriberto Coatl-Cuaya, and Antonio Rodríguez-Moreno
Department of Physiology, Anatomy and Cell Biology, Universidad Pablo de Olavide, Seville ES-41013, Spain

Spike timing-dependent plasticity (STDP) is a learning rule important for synaptic refinement and for learning and memory during development. While different forms of presynaptic t-LTD have been deeply investigated, little is known about the mechanisms of somatosensory cortex postsynaptic t-LTD. In the present work, we investigated the requirements and mechanisms for induction of developmental spike timing-dependent long-term depression (t-LTD) at L2/3-L2/3 synapses in the juvenile mouse somatosensory cortex. We found that postnatal day (P) 13–21 mice of either sex show t-LTD at L2/3-L2/3 synapses induced by pairing single presynaptic activity with single postsynaptic action potentials at low stimulation frequency (0.2 Hz) that is expressed postsynaptically and requires the activation of ionotropic postsynaptic NMDA-type glutamate receptors containing GluN2B subunits. In addition, it requires postsynaptic Ca^{2+}, Ca^{2+} release from internal stores, calcineurin, postsynaptic endocannabinoid synthesis, activation of CB_1 receptors, and astrocytic signaling to release the gliotransmitter D-serine to activate postsynaptic NMDARs to induce t-LTD. These results show direct evidence of the mechanism involved in developmental postsynaptic t-LTD at L2/3-L2/3 synapses, revealing a central role of astrocytes and their release of D-serine in its induction.

Key words: **astrocytes; D-serine; early postnatal development; juvenile; NMDAR; somatosensory cortex; spike timing-dependent plasticity; t-LTD**

Significance Statement

We show here the mechanisms and role of astrocytes and gliotransmitters in a postsynaptic spike timing-dependent long-term depression (t-LTD) form defined at layer (L)2/3-L2/3 synapses of the somatosensory cortex. We have discovered that this form of plasticity involves *N*-methyl D-aspartate receptors (NMDARs) containing the GluN2B subunit and requires astrocytes and the gliotransmitter D-serine to coactivate (together with glutamate) postsynaptic NMDAR to mediate LTD. This can be a general mechanism in the brain to define different forms of plasticity. Defining the mechanisms of synaptic plasticity may have important implications for brain repair, sensorial recovery, the treatment of neurodevelopmental disorders, and even, for educational policy.

Introduction

One of the most interesting properties of the mammalian brain is its ability to change in response to experience. This property, termed plasticity (Cajal, 1894; Mateos-Aparicio and Rodríguez-Moreno, 2019), is involved in the organization of cortical maps during development and in learning and memory processes (for review, Bliss et al., 2014; Magee and Grienberger, 2020). The most extensively studied forms of plasticity are long-term potentiation (LTP) and long-term depression (LTD) of synaptic transmission. Spike timing-dependent plasticity (STDP) is a Hebbian form of long-term synaptic plasticity found in all species studied, from insects to humans, and it is a strong candidate for a synaptic mechanism underlying circuit remodeling during development, as well as learning and memory (Debanne et al., 1994, 1998; Markram et al., 1997; Bi and Poo, 1998; Feldman, 2000; Martínez-Gallego et al., 2024; for reviews of STDP Feldman and Brecht, 2005; Dan and Poo, 2006; Campanac and Debanne, 2008; Caporale and Dan, 2008; Feldman, 2012; Brzosko et al., 2019; Martínez-Gallego et al., 2022a). In STDP,

Received April 30, 2024; revised Sept. 13, 2024; accepted Sept. 17, 2024.
Author contributions: Y.A.-R. designed research; Y.A.-T., J.S.-G., and H.C.-C. performed research; Y.A.-T., J.S.-G., H.C.-C., and A.R.-M. analyzed data; A.R.-M. wrote the paper.
This work was supported by the Spanish Agencia Estatal de Investigación and Fondo Europeo de Desarrollo Regional (FEDER, grants PID2019-107677GB-I00 and PID2022-136597NB-I00) and the Junta de Andalucía and FEDER (grant P20-0881) to A.R.-M. Y.A.-T was supported by a Marie Sklodowska-Curie Postdoctoral Fellowship (Horizon Europe program).
The authors declare no competing financial interests.
Correspondence should be addressed to Antonio Rodríguez-Moreno at arodmor@upo.es.
https://doi.org/10.1523/JNEUROSCI.0805-24.2024

the order and relative timing of pre- and postsynaptic action potentials (spikes) determine the direction and magnitude of the synaptic changes. Thus, timing-dependent LTP (t-LTP) occurs when a presynaptic spike is followed by a postsynaptic spike within milliseconds, whereas spike timing-dependent LTD (t-LTD) is induced when this order is reversed. t-LTP and t-LTD have been observed in neocortical slices (Sjöström et al., 2003; Bender et al., 2006; Nevian and Sakmann, 2006; Rodríguez-Moreno and Paulsen, 2008). STDP has been described at L4-2/3 and L2/3-L2/3 synapses at cortical areas; however, whereas the mechanisms of STDP have been extensively studied at L4-L2/3 neocortical synapses (Sjöström et al., 2003; Froemke et al., 2005; Bender et al., 2006; Nevian and Sakmann, 2006; Brasier and Feldman, 2008; Rodríguez-Moreno and Paulsen 2008; Rodríguez-Moreno et al., 2011, Min and Nevian, 2012, Martínez-Gallego et al., 2022b), comparatively much less is known about the cellular and molecular mechanisms of STDP at L2/3-L2/3 synapses.

Single STDP at L2/3-L2/3 synapses in the somatosensory cortex has been reported in juvenile animals (Banerjee et al., 2009, 2014; Feldman 2012, Brzosko et al., 2019 for review), but the exact cellular and molecular mechanisms involved in L2/3-L2/3 synapses of barrel cortex are not well known. To better understand the mechanisms of plasticity at these synapses, in the present work we studied the properties and mechanisms of t-LTD at L2/3-L2/3 synapses of young [postnatal day (P) 13–21] mouse somatosensory cortex using whole-cell patch-clamp recordings. We have chosen a P13–21 interval as it is a critical period of brain development during which much of refinement of synaptic connections occurs (Andrade-Talavera et al., 2023). We found that this form of NMDA receptor (NMDAR)-dependent t-LTD can be reliably induced by 100 pairings of postsynaptic spikes with single presynaptic activity at 0.2 Hz, and we confirmed that this LTD is postsynaptically expressed and demonstrated that it requires postsynaptic ionotropic GluN2B subunit-containing NMDARs, postsynaptic Ca^{2+}, Ca^{2+} release from internal stores, phosphatase calcineurin activation, postsynaptic endocannabinoid (eCB) synthesis and release, activation of CB_1 receptors, and astrocytic signaling, via release of the gliotransmitter D-serine.

Materials and Methods

Animals and ethical approval. All animal procedures were conducted in accordance with the European Union Directive 2010/63/EU regarding the protection of animals used for scientific purposes, and they were approved by the Ethics Committee of the Universidad Pablo de Olavide and the Ethics Committee of the Andalusian Government. C57BL/6 mice were purchased from Harlan Laboratories (Spain), and P13–21 mice of either sex were used. Animals were kept on a continuous 12 h light/dark cycle, at temperatures between 18 and 24°C, at 40–60% humidity, and with *ad libitum* access to food and water. In some experiments, dominant-negative (dn) SNARE mice (Pascual et al., 2005; Sardinha et al., 2017) of the same ages were used.

Slice preparation. Slices containing the barrel subfield of the somatosensory cortex were prepared as described previously (Agmon and Connors, 1991; Martínez-Gallego et al., 2022b). Briefly, mice were anesthetized with isoflurane (2%) and decapitated, and their whole brain was removed and placed in an ice-cold solution containing the following (in mM, 300 mOsm*L^{-1}): 126 NaCl, 3 KCl, 1.25 NaH_2PO_4, 2 $MgSO_4$, 2 $CaCl_2$, 26 $NaHCO_3$, and 10 glucose, pH 7.2. Slices (350 mm thick, Leica VT1000S Vibratome) were maintained oxygenated (95% O_2/5% CO_2) in the same solution for at least 1 h before use. Experiments were conducted at 33–34°C, during which the slices were perfused continuously with the solution indicated above.

Electrophysiological recordings. Slices containing the barrel cortex were identified and selected under a stereomicroscope. Two monopolar extracellular stimulation electrodes were placed at layer 2/3 of primary somatosensory cortex, just above the identified barrel. Whole-cell patch-clamp recordings were obtained from L2/3 pyramidal cells located in the same barrel column, between the two stimulation electrodes by using borosilicate glass pipettes that had a resistance of 5–7 MΩ when filled with (in mM, 290 mOsm*L^{-1}): 110 potassium gluconate, 40 HEPES, 4 NaCl, 4 ATP-Mg, and 0.3 GTP, pH 7.2–7.3. Cells with a pyramidal-shaped soma were selected for recording using infrared, differential interference contrast optics. The neurons were verified as pyramidal cells through their characteristic regular spiking responses to positive current injection. Whole-cell recordings were obtained with an Axon MultiClamp 700B amplifier (Molecular Devices). Only cells with a stable resting membrane potential below −55 mV were assessed, and the cell recordings were excluded from the analysis if the series resistance changed by >15% during the experiment. All recordings were low-pass filtered at 3 kHz and acquired at 10 kHz. The plasticity experiments were performed in current-clamp mode. To study plasticity, EPSPs were evoked alternately through two input pathways, test and control, each at 0.2 Hz, using brief current pulses (200 μs, 0.1–0.2 mA). Stimulation was adjusted to obtain an EPSP peak amplitude of 3–5 mV in control conditions, and pathway independence was ensured by the lack of cross-facilitation when the pathways were stimulated alternately at 40 ms intervals. Plasticity was assessed through the changes in the EPSP slope, measured in its rising phase as a linear fit between time points, corresponding to 25–30 and 70–75% of the peak amplitude under control conditions. To study tonic NMDAR current ($I_{tonicNMDAR}$; Le Meur et al., 2007), voltage-clamp recordings were performed holding at +40 mV in the presence of bicuculline (20 μM) and NBQX (10 μM). $I_{tonicNMDAR}$ was measured as changes in the holding current ($I_{holding}$) after D-AP5 (50 μM). Intracellular solution for voltage-clamp experiments contained the following: 120 CsCl, 8 NaCl, 1 $MgCl_2$, 0.2 $CaCl_2$, 10 HEPES, 2 EGTA, and 20 QX-314, pH 7.2 (290 mOsm). Astrocytes were identified by their morphology under differential interference contrast microscopy, eGFP fluorescence (astrocytes from dnSNARE mice), and were characterized by low membrane potential (−83 ± 0.5 mV; $n = 60$), low membrane resistance (22 ± 0.4 MΩ; $n = 60$), and passive responses (they do not show action potentials) to both negative and positive current injection.

Plasticity protocols. After establishing a stable basal EPSP over 10 min, the test input was paired 100 times with a single postsynaptic spike. The single postsynaptic spike (AP) was evoked by a brief somatic current pulse (5 ms, 0.1–0.5 pA). The control pathway was unstimulated during the pairing period. To induce t-LTD, the postsynaptic AP was evoked 18 ms before the onset of the EPSP. EPSP slopes were monitored for at least 30 min after the pairing protocol, and the presynaptic stimulation frequency remained constant throughout the experiment.

Pharmacology. The following compounds (in parenthesis catalog number identification) were purchased from Sigma-Aldrich: BAPTA (A4926), phenazine methosulfate (P9625), D-amino acid oxidase (A5222), as well as all the salts used to prepare the internal and external solutions. The following compounds were purchased from Tocris Bioscience: MK-801 maleate (0924), D-AP5 (0106), AM251 (1117), FK506 (3631), Ro 25-6981 maleate (1594), thapsigargin (1138), THL (3540), Zn^{2+} (3931), 7-chloro kynurenic acid sodium salt (3697), heparin (2812), ruthenium red (1439), bicuculline (0130), SCH50911 (0984), and NBQX (0373). The following compounds were purchased from Creative Diagnostics (913692690). These compounds were all dissolved in water except AM251, THL, AEA, and thapsigargin, which were dissolved in DMSO.

Data analysis. The data were analyzed with Clampfit 10.2 software (Molecular Devices), and the last 5 min of recording was used to estimate the changes in synaptic efficacy relative to the baseline. For the PPR experiments, two EPSPs were evoked for 30 s at the baseline frequency,

at the beginning of the baseline recording (40 ms apart), and again 30 min after the end of the pairing protocol. The PPR was expressed as the slope of the second EPSP divided by the slope of the first EPSP. A CV analysis was conducted on the EPSP slopes (Rodríguez-Moreno and Paulsen, 2008). The noise-free CV of the EPSP slopes was calculated as follows:

$$CV = \sqrt{\frac{\sigma^2(EPSP) - \sigma^2(noise)}{EPSP}},$$

where σ^2 (EPSP) and σ^2 (noise) are the variance of the EPSP and baseline, respectively. The plot compares the variation in the mean EPSP slope (M) to the change in response variance of the EPSP slope ($1/CV^2$). A comprehensive explanation can be found in Brock et al. (2020). Graphs were obtained using SigmaPlot 12.0.

Experimental design and statistical analysis. Animals were housed in small groups (3–5 mice). No randomization was performed to allocate subjects in the study. Animals were allocated arbitrarily. No exclusion criteria were predetermined. Experiments were conducted all day long. The study was not preregistered. For any comparisons between two groups a Mann–Whitney U test was used. For multiple comparisons to the same control, a Kruskal–Wallis test or a one-way ANOVA was used, with Holm−Sidak as a post hoc test. The data are expressed as mean ± SEM, and p values <0.05 were considered significant, $^*p < 0.05$, $^{**}p < 0.01$, $^{***}p < 0.001$.

Results

t-LTD can be induced by pairing single postsynaptic action potentials with presynaptic activity at low frequency in the mouse somatosensory cortex, is expressed postsynaptically, and requires postsynaptic ionotropic NMDARs containing the GluN2B subunit

First, we wanted to confirm that pairing presynaptic stimulation with single postsynaptic spikes at low frequency (0.2 Hz) is sufficient to induce t-LTD at L2/3-L2/3 synapses in juvenile mice. We monitored excitatory postsynaptic potentials (EPSPs) evoked by extracellular stimulation during whole-cell recording of L2/3 neurons in thalamocortical slices (P13–21). A post-before-pre pairing protocol (with a postsynaptic spike occurring ∼18 ms before presynaptic stimulation) induced robust t-LTD (68 ± 4%; $n = 8$; $p = 1.000$ vs baseline; Mann–Whitney U test), while an unpaired control pathway remained unchanged (101 ± 3%; $n = 8$; $p < 0.0001$ vs paired pathway; Mann–Whitney U test; Fig. 1*A–C*). We repeated the experiments in the presence of $GABA_A$ and $GABA_B$ receptor blockers (bicuculline, 10 μM and SCH50911, 20 μM, respectively) to determine whether they have a role in this form of t-LTD. In these experimental conditions, t-LTD was not affected, indicating that these receptors are not necessary for t-LTD induction (control t-LTD: 60 ± 8%, $n = 6$; bicuculline + SCH50911: 67 ± 9%, $n = 6$; $p = 0.5450$; two-tailed unpaired Student's t test; Fig. 1*D,E*). Thus, we performed the rest of experiments in the absence of any GABA receptor blocker. We next confirmed that this form of t-LTD is expressed postsynaptically as previously suggested (Banerjee et al., 2009, 2014). For this, we used different approaches. First, we estimated the noise-subtracted coefficient of variation (CV) of the synaptic responses before and after t-LTD induction. A plot of CV^{-2} versus the change in the mean evoked EPSP slope (M) before and after t-LTD yielded points around the horizontal line suggesting a postsynaptic expression (Brock et al., 2020; Fig. 1*F*). Second, in several experiments, we observed failures in synaptic transmission, and thus we analyzed whether a change in the number of failures occurred after t-LTD. No change in the number of failures after t-LTD was observed in our experiments (25 ± 4%, $n = 6$ after t-LTD vs 21 ± 3% in baseline, $n = 6$, $p = 0.485$; Mann–Whitney U test; Fig. 1*G*) also suggesting a postsynaptic locus of expression of this form of t-LTD. Finally, we analyzed the paired-pulse ratios (PPRs) during baseline and 30 min after a t-LTD pairing protocol was applied. The analysis of PPRs before and after t-LTD did not show changes of PPR after t-LTD (1.4 ± 0.1 after t-LTD, $n = 8$ vs 1.3 ± 0.2 during baseline, $n = 8$, $p = 0.279$; Mann–Whitney U test; Fig. 1*H*), which is also indicative of a postsynaptic locus. Together, these results are all indicative of a postsynaptic locus of expression for this form of t-LTD.

We next wanted to confirm the requirement of postsynaptic NMDARs for the induction of this form of t-LTD. In slices treated with the NMDAR antagonist D-2-amino-5-phosphonopentanoic acid (D-AP5), a post-before-pre pairing protocol failed to induce t-LTD (100 ± 7%, $n = 6$; vs interleaved control slices, in which t-LTD was clearly observed, 76 ± 8%, $n = 6$; $p = 0.032$; Kruskal–Wallis test followed by Holm–Sidak multiple-comparisons post hoc test; Fig. 1*I,J*). To confirm whether the NMDARs that are required for t-LTD are located postsynaptically and are ionotropic, we repeated the pairing experiments following the loading of the use-dependent NMDAR channel blocker MK-801 into the postsynaptic neuron via the recording patch pipette. Consistent with previous reports at neocortical synapses (Sjöström et al., 2003; Bender et al., 2006; Rodríguez-Moreno and Paulsen 2008; Rodríguez-Moreno et al., 2011; Banerjee et al., 2014), blocking postsynaptic NMDA receptors by including MK-801 (1 mM) in the recording pipette blocked the induction of t-LTD (106 ± 6%, $n = 6$; vs interleaved control slices, 76 ± 8%, $n = 6$; $p = 0.019$ Kruskal–Wallis test followed by Holm–Sidak multiple-comparisons post hoc test; Fig. 1*I,J*), supporting that postsynaptic ionotropic NMDARs are required for t-LTD induction. Next, we wanted to determine the subunit composition of these NMDARs. To test whether t-LTD is dependent upon GluN2A subunit-containing receptors, we used the GluN2A subunit-preferring antagonist Zn^{2+} (Bidoret et al., 2009). t-LTD was not affected in the presence of Zn^{2+} (300 nM; 67 ± 6%, $n = 6$, vs control slices, 72 ± 4%, $n = 6$; $p = 0.497$; Kruskal–Wallis test followed by Holm–Sidak multiple-comparisons post hoc test; Fig. 1*K,L*), indicating that the NMDAR involved in t-LTD do not contain GluN2A subunits. To further characterize the subunit composition of the NMDARs involved in t-LTD, we next investigated whether GluN2B subunit-containing NMDARs are necessary for the induction of t-LTD using the GluN2B subunit-selective non-competitive antagonist Ro 25-6981 (Fischer et al., 1997, Rodríguez-Moreno et al., 2010). Ro25-6981 (0.5 μM) prevented t-LTD induction (99 ± 3%, $n = 6$ vs interleaved control slices, 72 ± 4%, $n = 6$, $p = 0.001$; Kruskal–Wallis test followed by Holm–Sidak multiple-comparisons post hoc test; Fig. 1*K,L*), indicating that GluN2B subunit-containing NMDARs are required for t-LTD and suggesting that postsynaptic ionotropic GluN1/GluN2B subunits containing NMDAR are required for this form of t-LTD.

t-LTD requires postsynaptic Ca^{2+}, calcineurin and eCB signaling

Developmental t-LTD has been shown to require postsynaptic Ca^{2+} at L4-L2/3 synapses (Bender et al., 2006; Nevian and Sakmann 2006). We therefore investigated the postsynaptic Ca^{2+} requirement of t-LTD at L2/3-L2/3 synapses by loading the Ca^{2+} chelator BAPTA into the postsynaptic cell via the patch pipette. t-LTD was prevented when BAPTA (20 mM) was

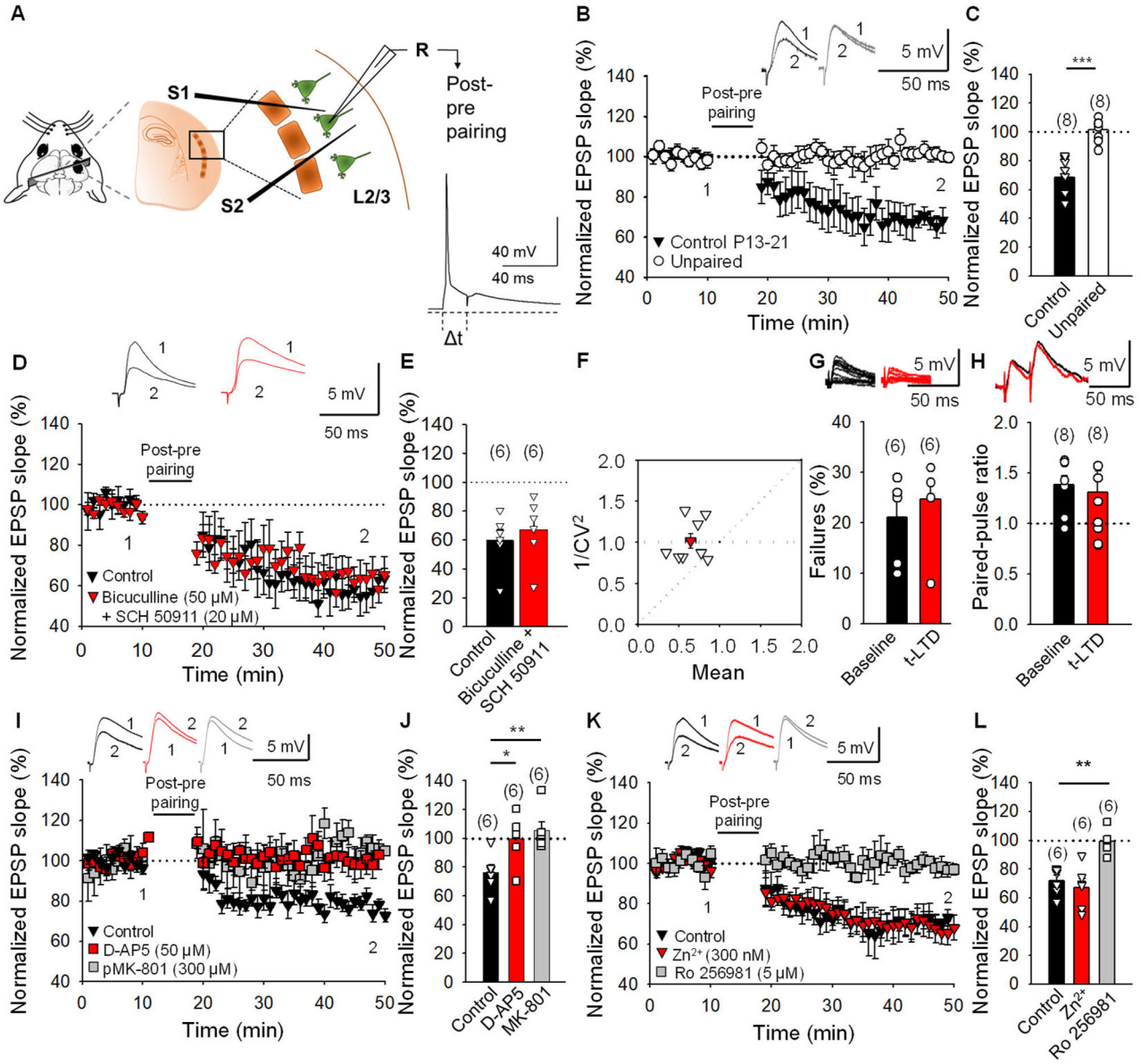

Figure 1. Input-specific STDP at L2/3-L2/3 synapses of the somatosensory cortex. ***A***, Schematic showing the general experimental setup. R, recording electrode. S1 and S1, stimulating electrodes. Inset, pairing protocol (*Δt*, time between the peak of the spike and the EPSP onset). ***B***, A post-before-pre single-spike pairing protocol induced t-LTD. The EPSP slopes monitored in paired (black symbols) and unpaired pathways (open symbols) are shown. Traces show EPSP before (1) and 30 min after (2) pairing. Depression was observed only in the paired pathway. ***C***, Summary of the results. t-LTD at L2/3-L2/3 synapses is postsynaptically expressed. ***D***, CV analysis is consistent with a postsynaptic expression of t-LTD. Normalized plot of CV^{-2} vs mean EPSP slope yielded points around the horizontal line following induction of t-LTD. ***E***, Number of failures did not change after t-LTD induction. Example traces during baseline and 30 min after induction of t-LTD are shown. ***F***, PPR did not change after t-LTD. Example traces during baseline and 30 min after induction of t-LTD are shown. t-LTD at L2/3-L2/3 synapses require postsynaptic ionotropic NMDAR containing the GluN2B subunit. ***G***, In the presence of D-AP5 or postsynaptic MK-801, t-LTD induction was prevented. The EPSP slopes monitored in D-AP5 (red symbols), MK-801-treated (gray symbols), and nontreated cells (black symbols) are shown. Traces show EPSP before (1) and 30 min after (2) pairing. ***H***, Summary of the results. ***I***, t-LTD induction was not prevented by bath application of Zn^{2+} but was completely prevented in the presence of Ro25-6981. The EPSP slopes monitored in the presence of Zn^{2+} (red symbols) and Ro25-6981 (gray symbols) are shown. Traces show EPSP before (1) and 30 min after (2) pairing. ***J***, Summary of the results. Error bars indicate SEM, and the number of slices is shown in parentheses. ***C***, ***G***, ***H***, Mann–Whitney *U* test. ***E***, Two-tailed unpaired Student's *t* test. ***J***, ***L***, Kruskal–Wallis test followed by Holm–Sidak multiple-comparisons test, $*p < 0.05$; $**p < 0.01$; $***p < 0.001$.

included in the recording pipette (99 ± 10%, $n = 6$, vs interleaved control slices, 61 ± 3%, $n = 16$, $p = 0.021$; Kruskal–Wallis test followed by Holm–Sidak multiple-comparisons post hoc test; Fig. 2*A*,*B*), indicating that t-LTD requires postsynaptic Ca^{2+} as it is expected if postsynaptic ionotropic NMDARs are required for its induction. It has previously been reported that Ca^{2+} channels and release of Ca^{2+} from intracellular stores are also required for t-LTD induction at neocortical synapses (Bender et al., 2006; Nevian and Sakmann 2006). To determine whether additional sources of calcium are necessary for t-LTD at L2/3-L2/3 synapses of the somatosensory cortex, we first repeated the pairing protocols following the application of the L-type Ca^{2+} channel blocker nimodipine loaded into the postsynaptic pipette; in the presence of nimodipine (10 μM), t-LTD induction was not affected (79 ± 7%, $n = 6$, vs interleaved control slices, 61 ± 3%, $n = 16$; $p = 0.1000$; Kruskal–Wallis test followed by Holm–Sidak multiple-comparisons post hoc test; Fig. 2*A*,*B*), indicating that Ca^{2+} passing through L-type VDCCs is not necessary for

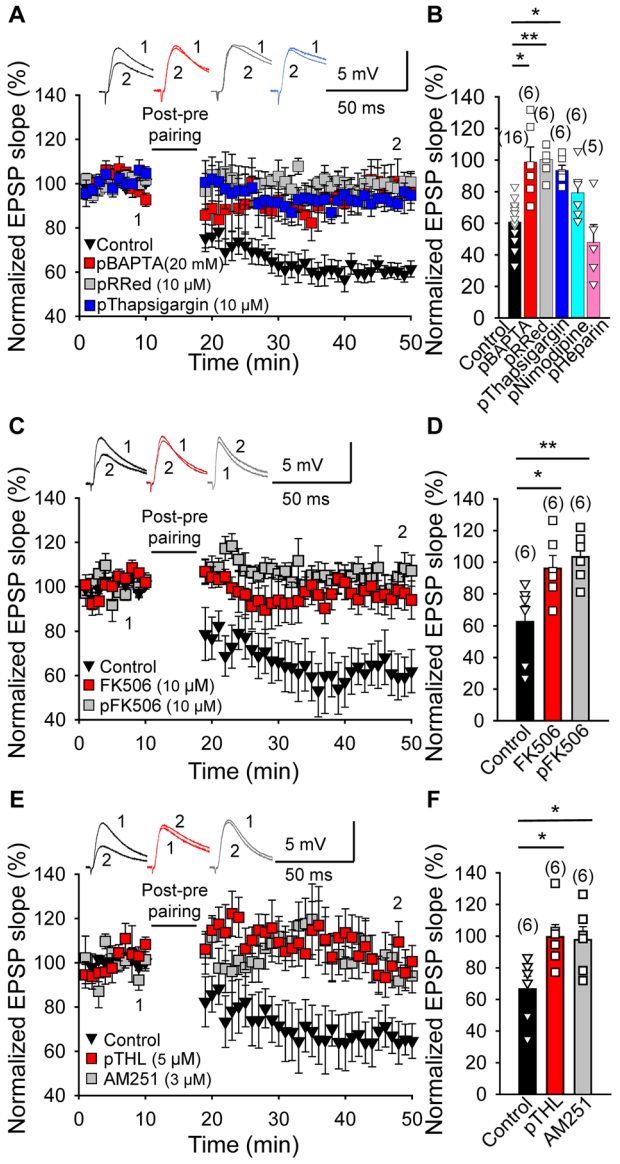

Figure 2. t-LTD requires postsynaptic calcium, calcineurin, and eCB signaling. ***A***, t-LTD was prevented by loading BAPTA, ruthenium red, or thapsigargin into the postsynaptic neuron via the recording pipette but not by nimodipine or heparin. The EPSP slopes monitored in control slices (black symbols) and in slices treated with BAPTA (red symbols), ruthenium red (gray symbols), or thapsigargin (blue symbols) are shown. Traces show EPSP before (1) and 30 min after (2) pairing. ***B***, Summary of the results. Postsynaptic calcineurin is involved in t-LTD at L2/3-L2/3 synapses. ***C***, Time course of effect of post-before-pre pairing in control conditions (black symbols) and in FK506-treated slices, bath applied (red symbols), or loaded into the postsynaptic cell via the patch pipette (gray symbols). Traces show EPSP before (1) and 30 min after pairing (2). ***D***, Summary of the results. ***E***, t-LTD requires activation of CB_1 receptors. Time course of t-LTD induction in control slices (black symbols) and in slices treated with THL and with AM251 following a post-before-pre pairing. Traces show EPSP before (1) and 30 min after pairing (2) in control slices (black symbols) and in slices treated with THL (red symbols) and AM251 (gray symbols). Note that in the presence of THL or AM251, t-LTD was completely prevented. ***F***, Summary of the results. Error bars indicate SEM, and the number of slices is shown in parentheses. Kruskal–Wallis test followed by Holm–Sidak multiple-comparisons test. $*p < 0.05$; $**p < 0.01$.

t-LTD. Next, we performed the t-LTD experiments in the presence of thapsigargin, which avoid refilling of intracellular Ca^{2+} stores after Ca^{2+} depletion; when thapsigargin (10 μM) was loaded into the postsynaptic cell, t-LTD was prevented (95 ± 5%, $n = 6$ vs interleaved control slices, 61 ± 3%, $n = 16$; $p = 0.021$; Kruskal–Wallis test followed by Holm–Sidak multiple-comparisons post hoc test; Fig. 2*A*,*B*). The presence of heparin (400U/ml), a blocker of IP_3R-mediated Ca^{2+} release (Ghosh et al., 1988), in the recording pipette did not prevent t-LTD induction (52 ± 15%, $n = 5$; vs interleaved control slices, 61 ± 3%, $n = 16$; $p = 0.1000$; Kruskal–Wallis test followed by Holm–Sidak multiple-comparisons post hoc test; Fig. 2*A*,*B*), suggesting that postsynaptic IP_3R-mediated Ca^{2+} release is not required for t-LTD. In contrast, inclusion in the patch pipette of ruthenium red (a blocker of ryanodine receptors) prevented t-LTD (100 ± 4%, $n = 6$; vs interleaved control slices, 61 ± 3%, $n = 16$, $p = 0.002$; Kruskal–Wallis test followed by Holm–Sidak multiple-comparisons post hoc test; Fig. 2*A*,*B*), suggesting that Ca^{2+} release from ryanodine-sensitive Ca^{2+} stores is required for this form of t-LTD. These results indicate a role for calcium in t-LTD induction. To gain mechanistic insight into how the activation of postsynaptic NMDA receptors could lead to t-LTD, we conjectured that a Ca^{2+}-dependent enzyme might be involved. Since the Ca^{2+}-dependent protein phosphatase calcineurin has earlier been implicated in other forms of LTD, both in the hippocampus (Mulkey et al., 1994) and neocortex (Torii et al., 1995; Rodríguez-Moreno et al., 2013), we tested the effect of the calcineurin inhibitor FK506 on L2/3-L2/3 t-LTD. We found that t-LTD was prevented when FK506 (10 μM) was bath applied (96 ± 8%, $n = 6$, $p = 0.013$; Kruskal–Wallis test followed by Holm–Sidak multiple-comparisons post hoc test; as it was prevented when was loaded into the postsynaptic neuron via a patch pipette (103 ± 6%, $n = 5$, vs 62 ± 10%, $n = 6$ in interleaved control slices, $p = 0.007$; Kruskal–Wallis test followed by Holm–Sidak multiple-comparisons post hoc test; Fig. 2*C*,*D*). These results indicate that the postsynaptic phosphatase calcineurin is involved in the induction of t-LTD at L2/3-L2/3 synapses.

eCBs are synthetized and released by postsynaptic cells in response to depolarization, Ca^{2+} elevation, and some synapses require signaling by eCBs for plasticity (for review, Noriega-Prieto et al., 2023). In a preliminary study (Banerjee et al., 2009), it has been suggested that CB_1Rs seem to be necessary for t-LTD at L2/3-L2/3 synapses of the mouse somatosensory cortex. To confirm this result and to add to the direct need of eCB synthesis, we performed t-LTD experiments with the postsynaptic neuron loaded, via the patch pipette, with tetrahydrolipstatin (THL, 5 μM), an inhibitor of the eCB synthesizing enzyme diacylglycerol lipase. In this experimental condition, t-LTD induction was completely prevented (99 ± 8%, $n = 6$, vs interleaved slices, 66 ± 8%, $n = 6$, $p = 0.023$; Kruskal–Wallis test followed by Holm–Sidak multiple-comparisons post hoc test; Fig. 2*E*,*F*), thus indicating that postsynaptic eCB synthesis is necessary for t-LTD. eCBs diffuse and activate CB_1 receptors on presynaptic neurons and/or glial cells (Sjöström et al., 2003; Navarrete and Araque, 2010, Min and Nevian 2012). To investigate the involvement of CB_1 receptors in L2/3-L2/3 t-LTD, we repeated the experiments in the presence of the CB_1 receptor antagonist AM251 (3 μM). In this condition, t-LTD was completely prevented (98 ± 8%, $n = 6$, vs interleaved slices, 66 ± 8%, $n = 6$, $p = 0.016$; Kruskal–Wallis test followed by Holm–Sidak multiple-comparisons post hoc test; Fig. 2*E*,*F*). Thus, t-LTD induction requires postsynaptic eCB synthesis and activation of CB_1 receptors.

t-LTD requires astrocyte signaling and D-serine

CB_1 receptors have been localized to presynaptic boutons (Chevaleyre et al., 2006 for review) and astrocytes (Navarrete and Araque, 2008; Min and Nevian, 2012). In astrocytes, CB_1 receptor activation has been suggested to stimulate the release

of glutamate and other gliotransmitters, including D-serine (Araque et al., 2014), and astrocytes have been involved in t-LTD and t-LTP at different synapses in the hippocampus and in the cortex (Min and Nevian, 2012; Rodríguez-Moreno et al., 2013; Rasooli-Nejad et al., 2014; Andrade-Talavera et al., 2016; Lalo et al., 2016; Pérez-Rodríguez et al., 2019; Pérez-Otaño and Rodríguez-Moreno, 2019; Falcón-Moya et al., 2020, Martínez-Gallego et al., 2022b). To investigate a possible involvement of astrocytes in the induction of t-LTD at L2/3-L2/3 synapses at P13–21, we loaded individual astrocytes, using the patch pipette, with the Ca^{2+} chelator BAPTA (20 mM) for 1–4 h before patching a pyramidal neuron. Ca^{2+}-dependent release of gliotransmitters is prevented by this treatment (Parpura and Zorec, 2010 and references therein). We recorded L2/3 neurons in the proximity (50–100 μm) of the BAPTA-loaded astrocyte and found that BAPTA loading of the astrocyte (aBAPTA) prevented the induction of t-LTD at L2/3-L2/3 synapses (100 ± 6%, $n = 6$ vs interleaved control slices, 65 ± 7%, $n = 6$, $p = 0.001$; one-way ANOVA followed by Holm–Sidak multiple-comparisons post hoc test; Fig. 3*A–C*).

We also assessed this phenomenon in dnSNARE mutant mice in which there is no functional vesicular gliotransmitter release (Pascual et al., 2005; Sardinha et al., 2017). In these mutant mice, the typical t-LTD observed in WT L2/3-L2/3 synapses (56 ± 6%, $n = 9$) was not present (101 ± 6%, $n = 6$, $p = 0.005$; ordinary one-way ANOVA followed by Holm–Sidak multiple-comparisons post hoc test vs WT; Fig. 3*D*,*E*). D-Serine has been proposed to be released by astrocytes by vesicular exocytosis and by nonvesicular mechanisms as BEST1 channel-mediated release (Koh et al., 2022). While our results using dnSNARE mice point out to a vesicular release of D-serine, to gain more insight into the release mechanism of D-serine, we repeated t-LTD experiments blocking exocytosis by treating the astrocytes (via the patch pipette) with the light chain of tetanus toxin (TeTxLC, 1 μM), which cleaves the vesicle-associated membrane protein, an indispensable part of the SNARE fusion complex. In this experimental condition, t-LTD was prevented (113 ± 8%, $n = 6$, vs 56 ± 6%, $n = 6$ in interleaved control slices, $p = 0.001$; ordinary one-way ANOVA followed by Holm–Sidak multiple-comparisons post hoc test; Fig. 3*D*,*E*), confirming that t-LTD requires SNARE-dependent exocytosis from astrocytes. Together, these results indicate that astrocytes are required for t-LTD induction at L2/3-L2/3 synapses of the somatosensory cortex.

These results also suggest that release of an astrocytic Ca^{2+}-dependent gliotransmitter is necessary for t-LTD induction. D-Serine, a coagonist at NMDA receptors, is a candidate gliotransmitter. D-Serine is synthesized in astrocytes and is released by glutamate receptor stimulation through a calcium- and SNARE-dependent exocytotic pathway (Mothet et al., 2000; 2005). In the CA1 region of the hippocampus, D-serine released by astrocytes has been demonstrated to modulate or mediate LTP (Henneberger et al., 2010; Zhuang et al., 2010). However, whereas D-serine has been proposed to modulate or mediate LTD in the same region, whether it is released by astrocytes has not been demonstrated (Zhang et al., 2008; Andrade-Talavera et al., 2016; Pérez-Rodríguez et al., 2019, Pinto-Duarte et al., 2019), and a direct release of D-serine from astrocytes with a role in t-LTD has not been demonstrated for the moment. To test whether D-serine might be responsible for the requirement of astrocytes during induction of postsynaptic t-LTD at L2/3-L2/3 synapses of the somatosensory cortex, we repeated the BAPTA loading experiments in the presence of D-serine (10–30 μM) added to the superfusion fluid. D-Serine without the pairing protocol produced a slight increase in EPSP slope [to 128 ± 9%, $n = 6$, $p = 0.0250$; ordinary one-way ANOVA followed by Holm–Sidak multiple-comparisons post hoc test vs baseline (100 ± 1.4%, $n = 6$); Fig. 3*C*]. In this experimental condition, t-LTD (absent in aBAPTA-treated slices: 100 ± 6%, $n = 6$) was completely recovered (64 ± 5%, $n = 6$, vs 65 ± 7%, $n = 6$ in interleaved control slices, $p = 0.973$; ordinary one-way ANOVA followed by Holm–Sidak multiple-comparisons post hoc test; Fig. 3*A–C*). We next performed the experiment in dnSNARE mice. When D-serine was added to the bath in dnSNARE mice, t-LTD (which was absent in these mice vs 65 ± 7%, $n = 6$ in WT control slices) was completely recovered (67 ± 4%, $n = 6$, vs 55 ± 8%, $n = 6$, $p = 0.1000$; ordinary one-way ANOVA followed by Holm–Sidak multiple-comparisons post hoc test; Fig. 3*D*,*E*). This result supports that the contribution of astrocytes during induction of t-LTD involves the release of a coagonist at NMDA receptors, most likely D-serine, as t-LTD, which is lost in the a-BAPTA and dnSNARE conditions, is completely restored in the presence of D-serine.

To investigate a possible mechanism involved in D-serine release, we repeated the experiments loading the astrocytes with the G-protein signaling blocker GDPβS and recorded neurons in the proximity. In this experimental condition, t-LTD was prevented (113 ± 11%, $n = 6$, vs interleaved control slices, 70 ± 9%, $n = 6$, $p = 0.913$; ordinary one-way ANOVA followed by Holm–Sidak multiple-comparisons post hoc test). The subsequent addition of D-serine recovered t-LTD (80 ± 5%, $n = 6$, $p = 0.551$; ordinary one-way ANOVA followed by Holm–Sidak multiple-comparisons post hoc test; Fig. 3*F*,*G*). This result suggests that a G-protein-dependent mechanism is involved in the astrocytic signaling required for t-LTD. Consistent with a role for CB_1 receptors in activating astrocytes, the addition of 10–30 μM D-serine also completely rescued t-LTD in the presence of the CB_1 receptor antagonist AM251 (69 ± 4%, $n = 6$ in nontreated (control) slices; 75 ± 7%, $n = 6$ in AM251 + D-serine-treated slices; 97 ± 4%, $n = 6$ in only AM251-treated slices; control vs AM251 $p = 0.013$, control vs AM251 + D-serine $p = 0.398$; ordinary one-way ANOVA followed by Holm–Sidak multiple-comparisons post hoc test; Fig. 3*H*,*I*). These results suggest that CB_1 receptors, probably located on astrocytes, are controlling astrocytic release of a coagonist (as D-serine) of postsynaptic NMDA receptors. If t-LTD requires eCB from the postsynaptic cell, to activate CB_1R located in the astrocytes, that are in turn activated by these receptors to release D-serine and bind to NMDAR to induce t-LTD, we reasoned that the direct activation of astrocytes by activating CB_1R with a cannabinoid (as anandamide, AEA), should mimic the effect of the t-LTD protocol. In fact, when we added AEA (500 nM) to the bath to activate CB_1R, an LTD of the EPSP was observed that was not present when AEA was applied when astrocytes were loaded with BAPTA (51 ± 9%, $n = 5$, vs 117 ± 8%, $n = 5$ in interleaved control slices, $p = 0.0006$; two-tailed unpaired Student's t test; Fig. 3*J*,*K*). These results are consistent with an astrocytic location of CB_1R.

To determine whether t-LTD needs binding of an agonist to the glycine/D-serine site of the NMDAR, we repeated the experiments in the presence of 10 μM 7-clorokinurenic acid (7-CK) that specifically blocks this binding site in the NMDAR and blocks NMDAR-mediated currents (to 8 ± 9%, $n = 5$). In this experimental condition, t-LTD was prevented (93 ± 7%, $n = 7$, vs 68 ± 7%, $n = 6$ in interleaved control slices, $p = 0.0301$; two-tailed unpaired Student's t test; Fig. 4*A*,*B*), indicating that the occupancy and activation of this site is necessary for t-LTD induction at L2/3-L2/3 synapses of the somatosensory cortex. To gain more insight on the need of astrocytes and the possible

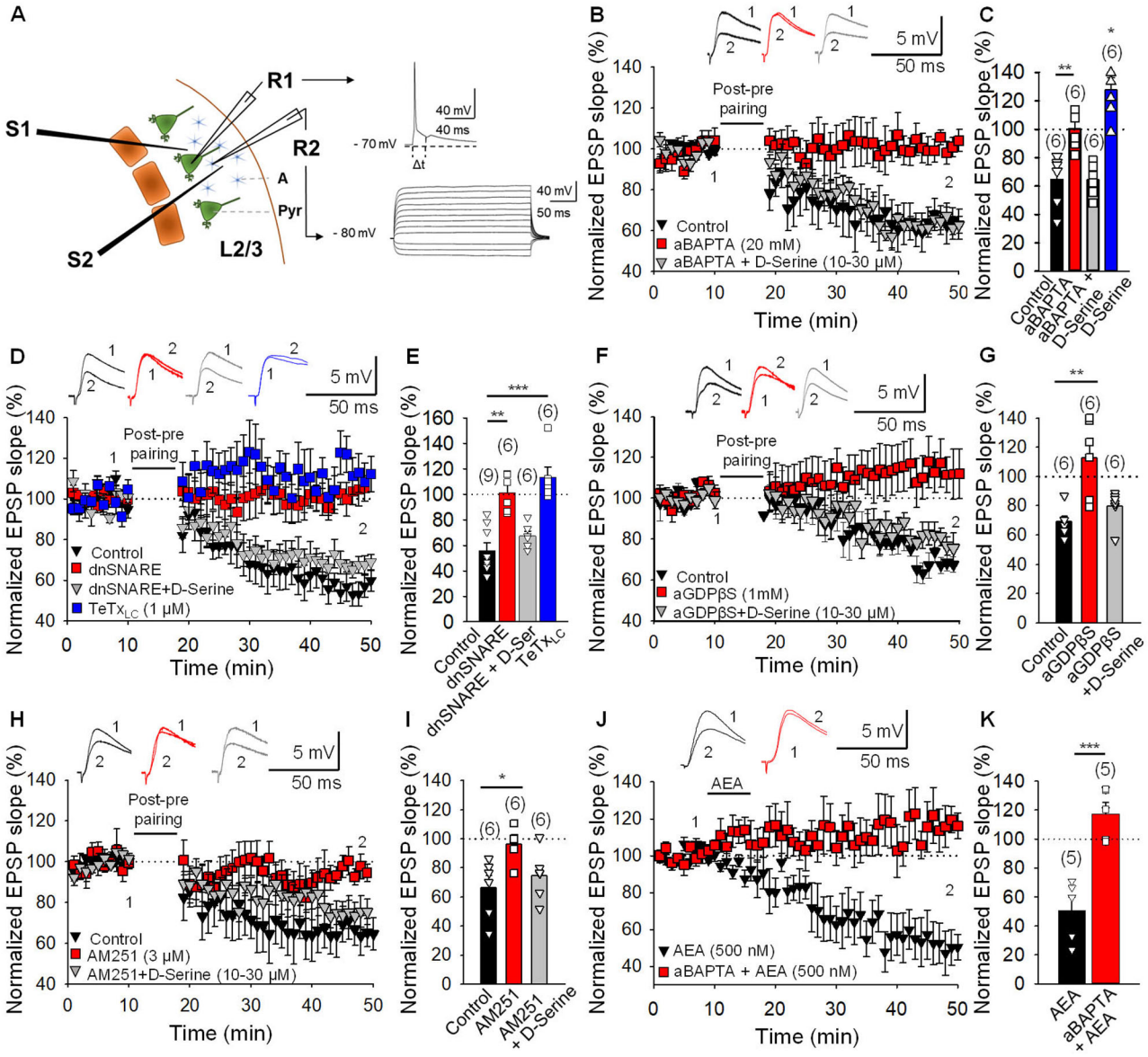

Figure 3. t-LTD at L2/3-L2/3 synapses requires astrocytes and D-serine. ***A***, Left, Scheme showing the general experimental setup: R1 and R2, recordings electrodes; S1 and S2, stimulating electrodes. Pyr, pyramidal neuron; A, astrocyte. Right, Voltage responses of an astrocyte shown in current clamp. ***B***, In astrocyte-neuron dual recordings with the astrocyte loaded with the calcium chelator BAPTA via the recording pipette (aBAPTA), a post-pre pairing protocol did not induce t-LTD. This t-LTD is recovered when D-serine is added to the superfusion fluid. The EPSP slopes monitored in control nontreated slices (black symbols), aBAPTA-treated astrocytes (red symbols), and aBAPTA + D-serine treated slices (gray symbols) are shown. The traces show the EPSP before (1) and 30 min after pairing (2). ***C***, Summary of the results. ***D***, t-LTD is not present in dnSNARE mutant mice or when astrocytes are treated with the light chain of the tetanus toxin ($TeTx_{LC}$) and is recovered in dnSNARE mice in the presence of D-serine. EPSP slopes monitored in control slices from WT animals (black symbols), in slices from dnSNARE mutant mice (red symbols), in slices from dnSNARE mice + D-serine (gray symbols), and in slices treated with $TeTx_{LC}$ (blue symbols) are shown. Traces from baseline (1) and 30 min after pairing protocol (2) are shown. ***E***, Summary of the results. ***F***, t-LTD is prevented by loading GDPβS into the astrocyte via the recording pipette (aGDPβS). In the presence of D-serine, t-LTD impaired with aGDPβS is recovered. The EPSP slopes monitored in control untreated slices (black symbols), in aGDPβS (red symbols), and in aGDPβS -treated cells with D-serine added to the perfusion fluid (gray symbols) are shown. Traces show the EPSP before (1) and 30 min after (2) pairing. ***G***, Summary of the results. ***H***, t-LTD induction is prevented in slices treated with AM251 (gray symbols) and is recovered when D-serine is added in AM251-treated slices. The EPSP slopes monitored in control untreated slices (black symbols), in AM251-treated slices (red symbols), and in AM251-treated slices with D-serine added to the perfusion fluid (gray symbols) are shown. Traces show the EPSP before (1) and 30 min after (2) pairing. ***I***, Summary of the results. ***J***, LTD of similar magnitude than t-LTD is induced by anandamide (AEA) in the bath (black symbols), an effect that was not present when astrocytes were treated with BAPTA via the patch pipette (red symbols). The EPSP slopes monitored in AEA-treated slices (black symbols) and in AEA-treated slices with astrocytes loaded with BAPTA (red symbols) are shown. Traces show the EPSP before (1) and 30 min after (2) AEA. ***K***, Summary of the results. Error bars indicate SEM, and the number of slices is shown in parentheses. ***C***, ***E***, ***G***, ***I***, Ordinary one-way ANOVA followed by Holm–Sidak multiple-comparisons post hoc test. ***K***, Two-tailed unpaired Student's *t* test. $*p < 0.05$; $**p < 0.01$; $***p < 0.001$.

astrocytic origin of D-serine for t-LTD at L2/3-L2/3 synapses, we performed dual recordings in astrocytes and neighboring pyramidal neurons, monitoring EPSP slopes evoked by basal stimulation at 0.2 Hz. Direct stimulation of astrocytes (depolarization from −80 to 0 mV at 0.4 Hz for 10 min; Min and Nevian, 2012) was sufficient to induce LTD (58 ± 10%, $n = 8$; Fig. 4*A*,*B*), which was not evident when astrocytes were stimulated in the presence of 7-CK (89 ± 5%, $n = 6$, $p = 0.039$; ordinary one-way ANOVA followed by Holm–Sidak multiple-comparisons post hoc test) or D-AP5(84 ± 7%, $n = 6$, $p = 0.031$; ordinary one-way

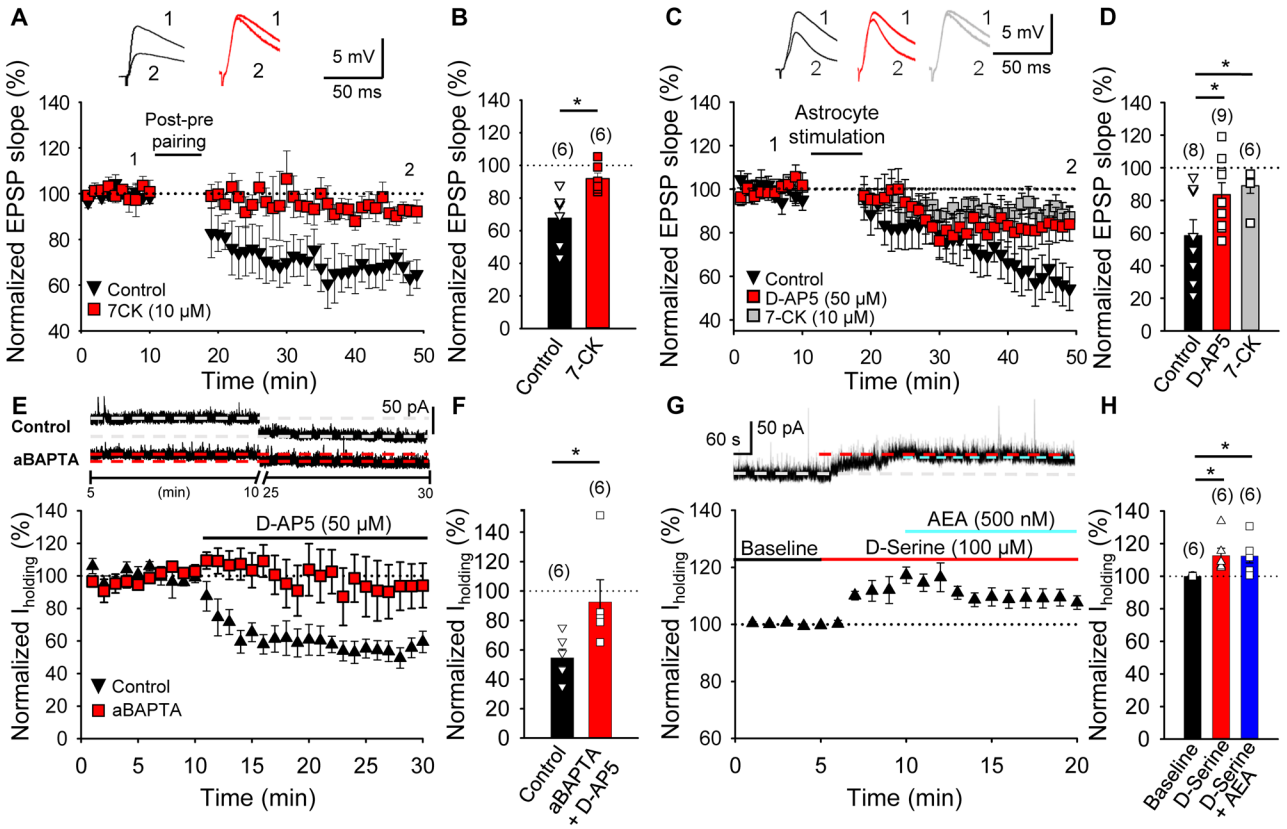

Figure 4. t-LTD requires NMDAR coagonist site occupancy by D-serine from astrocytes. ***A***, t-LTD is evident in nontreated slices, but cannot be induced when the slices are treated with 7-CK. The EPSP slopes monitored in control slices (black symbols) and in slices treated with 7-CK (red symbols) are shown. Traces show the EPSP before (1) and 30 min after (2) pairing. ***B***, Summary of the results. ***C***, Astrocyte stimulation (depolarization from −80 to 0 mV for 500 ms at 0.4 Hz) induced a robust t-LTD that was prevented in the presence of 7-CK. Time course of EPSP slope monitored from dual recordings performed in astrocytes and neighboring pyramidal neurons in untreated slices (black symbols) and in slices treated with 7-CK (red symbols) are shown. ***D***, Summary of the results. ***E***, $I_{tonicNMDAR}$ was significantly reduced by astrocytic Ca^{2+} chelation. The effect of D-AP5 in the holding current at +40 mV is shown in control slices (black symbols) and in slices with astrocytes loaded with BAPTA (red symbols). ***F***, Summary of the results (***G***) $I_{tonicNMDAR}$ increases in the present of D-serine (red) but not with the subsequent stimulation of astrocytes by AEA (cyan). The effect of AEA in the holding current at +40 mV (baseline) is shown in slices with the glycine/D-serine site saturated by D-serine (blue). ***H***, Summary of the results. Error bars indicate SEM, and the number of slices is shown in parentheses. ***B***, Two-tailed unpaired Student's *t* test, ***D***, Kruskal–Wallis test. ***F***, Mann–Whitney *U* test. ***H***, Repeated-measures one-way ANOVA followed by Holm–Sidak multiple-comparisons test. $*p < 0.05$; $**p < 0.01$.

ANOVA followed by Holm–Sidak multiple-comparisons post hoc test; Fig. 4*C*,*D*). To gain more insight into NMDAR modulation driven from astrocytes, we measured tonic NMDAR current ($I_{tonicNMDAR}$; Le Meur et al., 2007; Koh et al., 2022) performing voltage-clamp recordings holding at +40 mV in the presence of bicuculline (20 μM) and NBQX (10 μM). $I_{tonicNMDAR}$ was measured by the baseline shift (changes in $I_{holding}$) after D-AP5 (50 μM) in control slices and in slices with astrocytes loaded with BAPTA (20 mM). $I_{tonicNMDAR}$ was significantly reduced by astrocytic Ca^{2+} chelation (93 ± 15%, $n = 6$, vs 55 ± 6%, $n = 6$ in interleaved control slices, $p = 0.017$; Mann–Whitney *U* test; Fig. 4*E*,*F*), indicating that at S1 L2/3-L2/3 synapses, cortical astrocytes can regulate NMDAR tone in a Ca^{2+}-dependent manner. Together these results indicate that a gliotransmitter from astrocytes, as D-serine, activates (together with glutamate) postsynaptic NMDAR to produce t-LTD. As NMDAR tone can be attributed to glutamate and an NMDAR coagonist (as D-serine), to dissect the contribution of D-serine to NMDAR tone and its possible astrocytic origin, the NMDAR glycine/D-serine site was saturated by 100 μM D-serine (Papouin et al., 2017; Koh et al., 2022) and the $I_{tonicNMDAR}$ measured. In this condition, an increase of $I_{tonicNMDAR}$ was observed in the presence of D-serine (115 ± 5%, $n = 6$, $p = 0.035$; repeated-measures one-way ANOVA followed by Holm–Sidak multiple-comparisons post hoc test; Fig. 4*G*,*H*). The subsequent stimulation of astrocytes by AEA did not produce any increase in $I_{tonicNMDAR}$ (113 ± 4%, $n = 6$, $p = 0.952$; repeated-measures one-way ANOVA followed by Holm–Sidak multiple-comparisons post hoc test; Fig. 4*G*, *H*). Together, these data again suggest an astrocytic origin for D-serine modulating NMDAR that are necessary for t-LTD.

To further investigate the astrocytic origin of D-serine in response to astrocyte signal, we removed D-serine by treating the slices with 0.15 U/ml of D-amino-acid oxidase (DAAO), an enzyme that degrades dextro-amino acids or by blocking D-serine synthesis inside the astrocyte by using the serine racemase inhibitor phenazine methosulfate (Met-Phen; Beltrán-Castillo et al., 2017) loaded at 50 μM. In the first experimental condition (treating with DAAO), t-LTD induction was prevented (90 ± 10%, $n = 7$, vs control nontreated slices, 61 ± 7%, $n = 7$, $p = 0.0387$; two-tailed unpaired Student's *t* test; Fig. 5*A*,*B*). In addition, we performed experiments activating astrocytes with AEA in the presence of DAAO. We observed that LTD was induced with AEA in the absence but not in the presence of DAAO (60 ± 8%, $n = 6$, vs 99 ± 1%, $n = 6$, $p = 0.004$; two-tailed unpaired Student's *t* test; Fig. 5*C*,*D*), again suggesting that D-serine is of astrocytic origin. In the second experimental condition (Met-Phen), t-LTD was not affected (51 ± 7%, $n = 6$, vs control nontreated slices t-LTD: 60 ± 8%, $n = 6$, $p = 0.368$; two-tailed

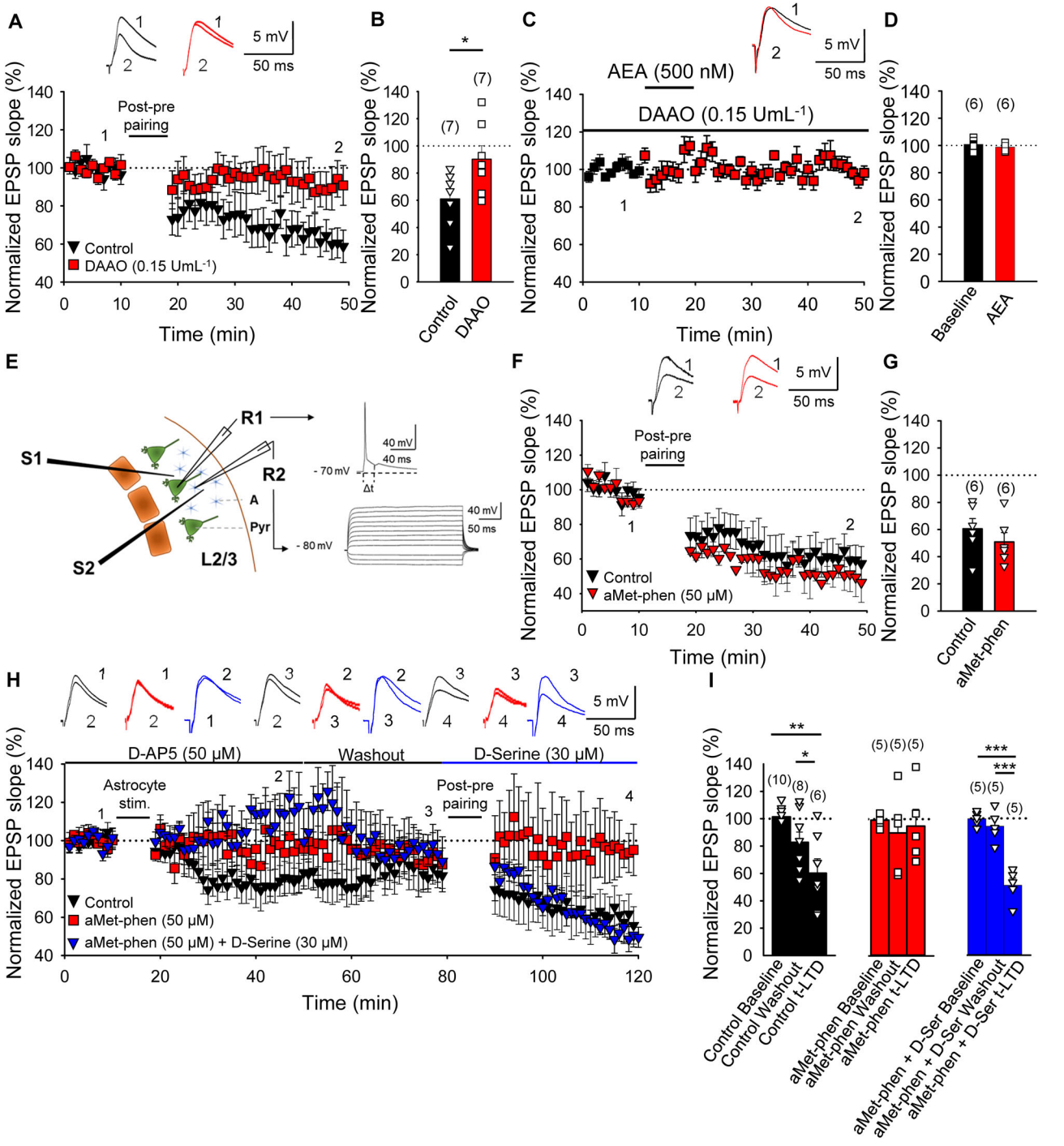

Figure 5. D-Serine required for t-LTD is released by astrocytes. ***A***, t-LTD is prevented in slices treated with DAAO. Time course of EPSP slope monitored in control untreated slices (black symbols) and in slices treated with DAAO (red symbols) are shown. Traces show the EPSP before (1) and 30 min after (2) pairing. ***B***, Summary of the results. ***C***, LTD induced by AEA is prevented in slices treated with DAAO. Time course of EPSP slope monitored in slices treated with DAAO (red symbols) are shown. Traces show the EPSP before (1) and 30 min after (2) AEA. ***D***, Summary of the results. ***E***, Scheme showing the dual recording experimental setup: R1 and R2, recordings electrodes; S1 and S2, stimulating electrodes. Pyr, pyramidal neuron; A, astrocyte. ***F***, t-LTD is not prevented when astrocytes are treated with phenazine methosulphate (aMet-phen). Time course of EPSP slope monitored in control untreated slices (black symbols) and in slices with astrocytes treated with aMet-phen (red symbols) is shown. Traces show the EPSP before (1) and 30 min after (2) pairing. ***G***, Summary of results. ***H***, t-LTD is suppressed by intra-astrocyte phenazine methosulfate after depletion of D-serine with astrocyte stimulation in the presence of D-AP5 and the addition of D-serine to the bath recovers t-LTD. Time course of EPSP in control slices (black symbols), in slices with astrocyte treated with Met-phen before and after depletion of D-serine (red symbols), and in slices with astrocyte treated with Met-Phen with D-serine added to the bath during the t-LTD protocol is shown. The traces show the EPSP before (1), 30 min after astrocyte stimulation in presence of D-AP5 (2), after 30 min of washout of D-AP5, before (3), and 30 min after pairing (4). ***I***, Summary of results. Error bars indicate SEM, and the number of slices is shown in parentheses. ***B***, ***D***, ***G***, Two-tailed unpaired Student's *t* test; ***I***, one-way repeated-measures ANOVA followed by Holm–Sidak multiple-comparisons test. $*p < 0.05$; $***p < 0.001$.

unpaired Student's *t* test; Fig. 5*E–G*). As this compound does not interfere with D-serine that is already stored in the astrocyte, it is possible that t-LTD is in fact induced by the D-serine that is stored into the astrocyte before the racemase addition. To clarify this point, we repeated the experiments in conditions in which the stored D-serine is depleted (by direct astrocyte stimulation as in

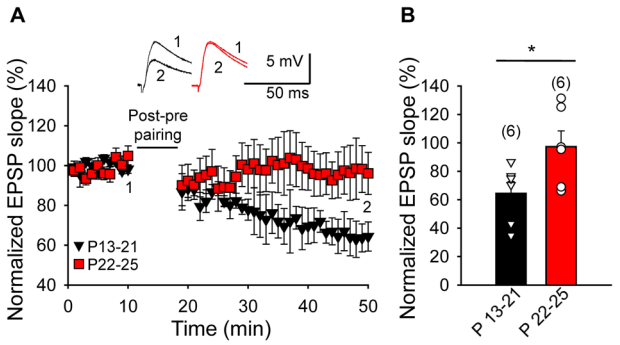

Figure 6. Developmental profile of t-LTD at L2/3-L2/3 synapses of the mouse somatosensory cortex. t-LTD is evident during the second and third week of development but cannot be induced during the fourth week. ***A***, The EPSP slopes monitored at P13–21 (black symbols) and at P22–25 (red symbols) are shown. Traces show the EPSP before (1) and 30 min after (2) pairing. ***B***, Summary of the results. Error bars indicate SEM, and the number of slices is shown in parentheses. Mann–Whitney *U* test. $*p < 0.05$.

Fig. 5*A*,*B*) in the presence of D-AP5 to avoid t-LTD induction by depleted D-serine. Then we washed-out D-AP5 and applied the t-LTD protocol. In this experimental condition no t-LTD was observed when slices were treated with Met-Phen (95 ± 10%, $n = 5$, $p = 0.713$; one-way repeated-measures ANOVA), whereas the same protocol with no Met-Phen loaded produced clear t-LTD (60 ± 6%, $n = 6$, $p = 0.004$; one-way repeated-measures ANOVA followed by Holm–Sidak multiple-comparisons post hoc test; Fig. 5*H*,*I*). Interestingly, when the slices were treated with Met-Phen and no t-LTD was observed, the addition of D-serine to the bath recovered t-LTD (94 ± 5%, $n = 5$, vs 51 ± 5%, $n = 5$ in interleaved control slices, $p < 0.001$; one-way repeated-measures ANOVA followed by Holm–Sidak multiple-comparisons post hoc test; Fig. 5*H*,*I*). These results again suggest that astrocytic D-serine is involved in t-LTD induction.

Loss of t-LTD during the fourth week of development

We studied the age profile of this form of t-LTD and found that t-LTD can be induced until P21 (64 ± 8%, $n = 6$; Fig. 6), disappearing thereafter in the fourth week of development (at P22–25, 97 ± 11%, $n = 6$, $p = 0.0040$ vs t-LTD at P13–P21; Mann–Whitney *U* test; Fig. 6). Hence, this form of t-LTD is related to a specific developmental period, as it is not induced after that.

Discussion

We have found here that t-LTD at somatosensory L2/3-L2/3 synapses of juvenile mice is postsynaptically expressed and requires postsynaptic ionotropic NMDARs containing GluN1/GluN2B subunits for its induction. This form of t-LTD requires postsynaptic Ca^{2+} and Ca^{2+} release from internal stores, postsynaptic eCB synthesis, activation of CB1 receptors, and astroglial signaling. Furthermore, the NMDA receptor coagonist D-serine is required for t-LTD, and this D-serine is released by astrocytes (Fig. 7). This form of somatosensory cortex t-LTD is in some aspects similar to t-LTD at layer 4-to-layer 2/3 synapses in neocortex as both require NMDAR and astrocyte signaling (Bender et al., 2006; Nevian and Sakmann, 2006; Rodríguez-Moreno and Paulsen, 2008) but differ in important aspects, as the locus of expression of the t-LTD and the location of the NMDAR required; whereas t-LTD at L2/3-L2/3 synapses is postsynaptically expressed and requires postsynaptic NMDAR, t-LTD at L4-L2/3 synapses is expressed presynaptically and requires presynaptic NMDARs (Rodríguez-Moreno and Paulsen, 2008). While both forms of t-LTD require astrocytes for their induction, interestingly, in the case of layer 4-to-layer 2/3 synapses the gliotransmitter released by astrocytes to activate presynaptic NMDARs is glutamate (Min and Nevian, 2012), while at L2/3-L2/3 synapses the gliotransmitter is D-serine acting on postsynaptic ionotropic NMDA receptors.

t-LTD is expressed postsynaptically and requires postsynaptic ionotropic NMDARs containing the GluN2B subunit

We used three different approaches to confirm the locus of expression of this form of t-LTD, and all the three, fluctuation analysis (including failure rate), and PPR were consistent with postsynaptic changes, strongly suggesting that the locus of expression of this cortical form of t-LTD is postsynaptic. We also confirmed that this t-LTD requires postsynaptic ionotropic NMDA receptors as it was prevented by the inclusion of the NMDA receptor antagonist MK801 into the postsynaptic neuron, but an additional role for a postsynaptic NMDA receptor-mediated metabotropic effect cannot be completely ruled out (Nabavi et al., 2013). The presence of different subpopulations of NMDA receptors in different brain regions suggests that different subtypes play different roles in brain function (Paoletti et al., 2013). Here, we used different antagonists to determine the subunit composition of the NMDARs involved in this form of postsynaptic t-LTD. In our experiments at L2/3-L2/3 synapses, we have previously shown that NMDAR responsible for t-LTD included GluN2B subunits but not GluN2C/2D subunits (Banerjee et al., 2009) consistent with the data we have obtained. Here, we also demonstrate that these receptors do not contain GluN2A subunits, as t-LTD is not prevented in the presence of the GluN2A subunit-containing NMDAR antagonist Zn^{2+}, thus suggesting that the composition of these receptors is GluN1/GluN2B. A possible role of GluN3 subunits require further investigation (Paoletti et al., 2013). The t-LTD characterized here requires GluN2B-containing NMDARs that are known to be involved in LTD also at other synapses, for instance they are involved in LTD at CA3-CA1 hippocampal synapses (Papouin et al., 2012). GluN2B-containing NMDARs play critical roles in cognitive functions in rodent that are thought to be mediated by their roles in LTD (Brigman et al., 2010). For instance, impairment of fear extinction learning in rats by a GluN2B-containing NMDAR antagonist is associated with their impaired LTD in the amygdala (Dalton et al., 2012), while enhancement of spatial reversal learning in mice by NMDAR coagonist D-serine is associated with their enhanced LTD in the hippocampus (Duffy et al., 2008). Consistent with our data, in the somatosensory cortex, GluN2B-KO mice exhibit neonatal lethality, impaired somatosensory synapse refinement, and impaired LTD (Kutsuwada et al., 1996). It is well established that NMDARs are located at both synaptic and extrasynaptic regions, with extrasynaptic NMDARs activated by spillover of synaptic glutamate or glutamate released from glia (Haydon and Carmignoto, 2006), and synaptic NMDARs activated only by synaptically released glutamate. There are accumulating evidences that GluN2A subunit-containing NMDARs are more likely to be concentrated at synapses, whereas GluN2B- and GluN2C/2D-containing NMDARs are more enriched at extrasynaptic sites in excitatory neurons (Zhou and Sheng, 2013). While the t-LTD characterized here involves GluN2B subunit-containing NMDAR and their location is probably extrasynaptic, more work is necessary to determine the synaptic and/or extrasynaptic location of these receptors.

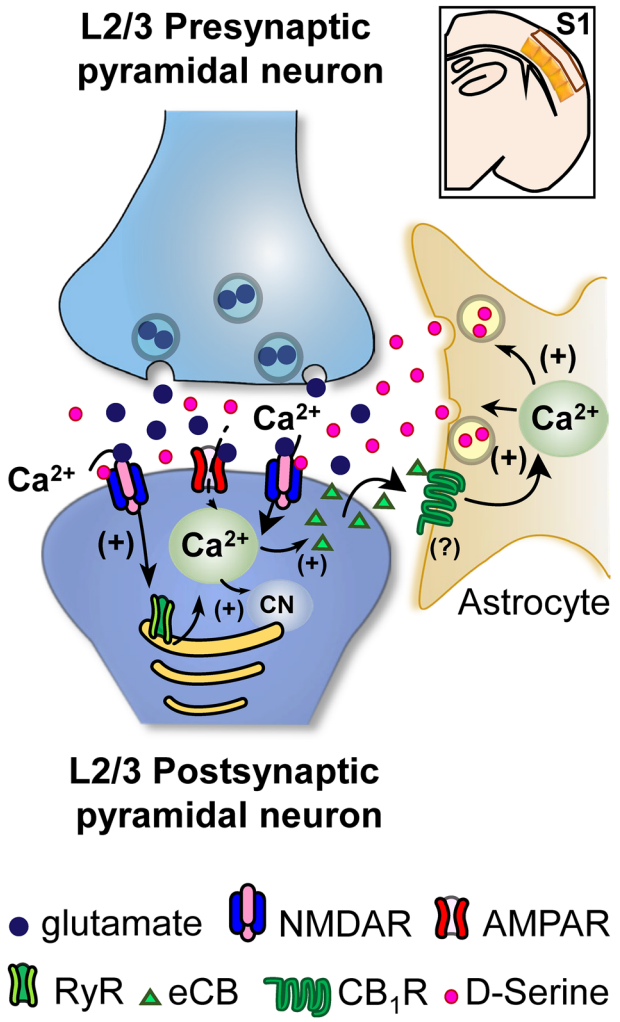

Figure 7. Model of postsynaptic developmental t-LTD at L2/3-L2/3 synapses of the primary somatosensory cortex (S1). t-LTD is induced by a post-before-pre, single-spike pairing protocol at P13–21. Presynaptically released glutamate activates postsynaptic NMDA receptors, which permeates Ca^{2+} into the postsynaptic neuron, causing calcineurin activation and Ca^{2+} release from internal stores in a Ca^{2+}-dependent Ca^{2+} release manner, driving eCBs synthesis and release. The eCB signal leads to the activation of CB_1 receptors possibly situated in surrounding astrocytes, facilitating D-serine release from astrocytes, which, together with glutamate released from presynaptic neurons, activates postsynaptic NMDA receptors on L2/3 postsynaptic neurons to induce t-LTD.

Calcineurin is necessary for t-LTD induction

Protein phosphatases, including calcineurin, have been reported to be required for several different forms of LTD, both in the hippocampus (Mulkey et al., 1994) and neocortex (Torii et al., 1995). Using FK506 to block calcineurin activity, our results indicate the involvement of postsynaptic calcineurin in t-LTD induction. A similar requirement of calcineurin (but presynaptic) has been also described for t-LTD in the hippocampus (Andrade-Talavera et al., 2016) and in neocortical pattern-dependent LTD (p-LTD; Rodríguez-Moreno et al., 2013).

Ca^{2+} and eCBs and CB1 receptor requirements for t-LTD

We found that t-LTD requires a rise in postsynaptic Ca^{2+}, as it was blocked by the presence of BAPTA into the postsynaptic cell. Interestingly, Ca^{2+} entering into the postsynaptic neuron trough L-type VDCC is not necessary for this t-LTD as it is not prevented or affected in the presence of nimodipine. Thus, Ca^{2+} is most probably passing through NMDAR channels, as postsynaptic ionotropic NMDAR are required for this t-LTD. It also requires Ca^{2+} from intracellular stores as compounds that affect intracellular Ca^{2+} dynamics as thapsigargin (that avoid refilling of intracellular stores after depletion) or ruthenium red (that blocks RyR receptors and thus Ca^{2+} release to the cytoplasm) blocked t-LTD induction. Interestingly, IP_3R are not required as blocking these receptors by heparin did not affect t-LTD induction. This form of t-LTD thus resembles previously described postsynaptic NMDA receptor-dependent forms of LTD (Mateos-Aparicio and Rodríguez-Moreno, 2020). Postsynaptic loading of THL, a selective inhibitor of the eCB synthesizing enzyme diacylglycerol lipase, blocked the induction of t-LTD, suggesting that eCBs are involved in the induction of t-LTD. In our experiments, AM-251, an eCB CB_1 receptor antagonist, prevented the induction of t-LTD, suggesting that eCB binding to CB_1 receptors is required for induction of t-LTD. CB_1 receptors involved in synaptic plasticity are located in the presynaptic neuron (Sjöström et al., 2003) and/or in astrocytes (Navarrete and Araque, 2008, 2010; Min and Nevian, 2012). In the present work, we did not elucidate the site of CB_1 receptors mediating t-LTD and further work will be required to unequivocally address this question, although the demonstration that astrocytes are required for t-LTD and that AEA stimulation gives rise to LTD but not when astrocytes are loaded with BAPTA is suggestive that astrocytic CB_1 receptors might be involved.

Astrocytes are required for induction of t-LTD

Through three different approaches, we demonstrated the involvement of astrocytes in postsynaptic t-LTD observed at P13–21 mice. First, introducing BAPTA into astrocytes completely prevented t-LTD induction. Second, vesicular release is impaired in dnSNARE mice, and third, when light chain tetanus toxin is loaded into astrocytes, t-LTD is prevented, and t-LTD is not observed in slices from these animals, indicating that Ca^{2+}-regulated release of a gliotransmitter is necessary for t-LTD induction at somatosensory L2/3-L2/3 synapses. A role for astrocytes in synaptic depression is established. For instance, ATP released from astrocytes because of neuronal activity can modulate synaptic transmission in cultured hippocampal neurons; and ATP tonically suppresses glutamatergic transmission via P2Y receptors, an effect that depends on the presence of co-cultured astrocytes (Zhang et al., 2003). Glutamate activates non-NMDA receptors on astrocytes and triggers ATP release which causes homo- and heterosynaptic depression (Zhang et al., 2003). In addition, astrocytes have been involved in LTD in the CA1 region of the hippocampus (Andersson et al., 2007, Han et al., 2012; Navarrete et al., 2019) and in other brain regions as the cerebellum (Sasaki et al., 2012), or the supraoptic nucleus (Panatier et al., 2006, Durkee et al., 2021 for a review of roles of astrocytes in LTD). In STDP, astrocytes have been involved in t-LTD in the hippocampus (Andrade-Talavera et al., 2016; Pérez-Rodríguez et al., 2019, Falcón-Moya et al., 2020), the striatum (Valtcheva and Venance, 2016), and at L4-L2/3 synapses of the somatosensory cortex (Min and Nevian, 2012; Rodríguez-Moreno et al., 2013; Martínez-Gallego et al., 2022b). Here we add to this knowledge and demonstrate for the first time a role of astrocytes at L2/3-L2/3 synapses of somatosensory cortex.

D-Serine recovers t-LTD, modulates postsynaptic NMDARs, and is released from astrocytes

Indeed, we found that the addition of D-serine to the superfusion fluid completely restored t-LTD in experiments in which astrocytes

were loaded with BAPTA and in dnSNARE mutants, suggesting that astrocytes release a gliotransmitter required for t-LTD, acting as coagonist on postsynaptic NMDARs. From our results, it is clear that D-serine is released by SNARE-dependent exocytosis as indicated by dnSNARE results and by direct loading of astrocytes with the light chain of tetanus toxin, which blocks exocytosis. Additionally, D-serine recovered t-LTD when astrocytes were loaded with GDPβS and when AM251 was added in the superfusion fluid. These results are all consistent with the possible location of CB_1 receptors on the astrocytes and with the fact that D-serine is released from astrocytes to act on postsynaptic NMDARs involved in t-LTD. The fact that racemase inhibition together with D-serine depletion prevents t-LTD is directly consistent with the astrocytic origin of D-serine (Henneberger et al., 2010) as are the results obtained when the slices were treated with DAAO and astrocytes were stimulated. The evaluation of NMDAR-tonic currents, which are directly affected by astrocytic chelation (with BAPTA), indicate that S1 L2/3-L2/3 cortical astrocytes can regulate NMDAR tone in a Ca^{2+}-dependent manner. In addition, from our results it is clear that D-serine released from astrocytes binds to postsynaptic NMDARs that mediate t-LTD at L2/3-L2/3 synapses but the possibility that any other activator of the glycine site of the NMDAR may produce the same effect exists, for instance, glycine or/and D-alanine released from astrocytes may affect t-LTD, and more experiments are needed to clarify this point. In STDP, these results are, in principle, similar to some of the results found for t-LTD in the hippocampus at CA3-CA1 synapses, but taken into account one important difference that NMDARs involved in t-LTD in the hippocampus are presynaptic (Andrade-Talavera et al., 2016). Thus, it is important to note that our results show that D-serine released by astrocytes may act on both pre- and postsynaptic NMDARs to mediate t-LTD. D-Serine from astrocytes has also been previously involved in postsynaptic LTP induced with high-frequency stimulation (Henneberger et al., 2010), but whether it may be also involved in presynaptic LTP forms remains to be determined. Thus, D-serine from astrocytes has been demonstrated to be required for presynaptic t-LTD in the hippocampus (Andrade-Talavera et al., 2016) and for postsynaptic t-LTD at L2/3-L2/3 synapses of the somatosensory cortex (present work). Interestingly, as a novelty, we show here for the first time that D-serine is acting on postsynaptic NMDARs to mediate a postsynaptic form of LTD at the somatosensory cortex and we show the first evidence that D-serine involved in a postsynaptic form of t-LTD is directly released by astrocytes.

What is the physiological role of this form of plasticity?

For the moment, the exact role of STDP in the somatosensory cortex is not known, and more work is necessary to specifically determine functions for t-LTP and t-LTD. STDP seems a good candidate to mediate spatial learning in the hippocampus (Bush et al., 2010) and the possible role of t-LTP and t-LTD in forms of learning involving the hippocampus and the somatosensory cortex whisker discrimination will be addressed in future studies. Our studies were done in developing P13–P21 animals, and the form of postsynaptic t-LTD described here is present during the second and third week of development and is absent after P22 indicating its relevance during maturation. The functions of t-LTP and t-LTD during development are most probably related to the refinement of synaptic connections and remodeling of neuronal circuits (Andrade-Talavera et al., 2023). As a Hebbian learning rule, t-LTP should occur when the spike order is pre-before-post, strengthening those connections in which the presynaptic neuron takes part in firing the postsynaptic cell, as predicted by Hebb, whereas t-LTD occurs when the spike order is reversed, so that noncausal spiking weakens the connections involved, possibly as a first step in the elimination of those connections during development as has been suggested (Caporale and Dan, 2008). Indeed, further studies will be necessary to determine the true influence of STDP in the barrel cortex and the specific developmental role of t-LTD and t-LTP in these circuits. As discussed previously (Pérez-Rodríguez et al., 2019; Falcón-Moya et al., 2020), t-LTD most probably participates in refining synapses during the first postnatal weeks of development, potentially weakening excitatory synapses that are underused or behaviorally irrelevant (Buonomano and Merzenich, 1998; Feldman and Brecht, 2005).

It is interesting to note that with these new results it is clear that both pre- and postsynaptic forms of t-LTD in young animals may require D-serine from astrocytes (presynaptic t-LTD at CA3-CA1 synapses in the hippocampus and postsynaptic t-LTD at L2/3-L2/3 in the somatosensory cortex) in the same animals. Presynaptic plasticity may involve structural changes and may change the short-term properties of neurotransmitter release, participating in circuit computations, and changing the excitatory/inhibitory balance or sensory adaptations (Monday et al., 2018). Why some synapses, like L4-L2/3 synapses (and as observed in the hippocampus), show pre- and/or postsynaptic plasticity requires further study. Interestingly, in the somatosensory cortex, t-LTD of L4-L2/3 and L2/3-L2/3 synapses have different requirements, indicating that the pre- or postsynaptic expression of plasticity is fundamental for the correct functioning of brain circuits and that it is possible they are regulated differently (Banerjee et al., 2009, 2014). Presynaptically expressed forms of t-LTD may control the trial-to-trial reliability, and along with the postsynaptically expressed t-LTD, they may induce a larger change in signal-to-noise ratio than postsynaptic changes alone, as described in the auditory cortex (Froemke et al., 2013). In addition, different sites of expression may be an advantage to the system as it may offer more possibilities for plasticity when one is disrupted. Finally, while technically challenging, it is becoming possible to associate particular behaviors with a particular locus of plasticity thanks to improved tools to specifically manipulate LTD processes in vivo (Nabavi et al., 2014). Astrocytes and D-serine have been associated with behavior in the hippocampus, where the lack of IP_3R_2 produced remote recognition, fear, and spatial memories impairments, and these animals showed a deficit in LTD that was recovered by supplementation of D-serine (Pinto-Duarte et al., 2019). Also in the hippocampus, impairing glial functions with fluoroacetate reduced the magnitude of LTD, which was restored by exogenous D-serine, and interestingly, this D-serine enhanced spatial memory retrieval and rescued fluoroacetate-induced impairment of memory retrieval, suggesting links between LTD and spatial memory retrieval (Zhang et al., 2008). Notwithstanding this, the potential behavioral influence of the postsynaptic form of LTD studied here is still an emerging issue of particular interest in the near future.

References

Agmon A, Connors BW (1991) Thalamocortical responses of mouse somatosensory (barrel) cortex in vitro. Neuroscience 41:365–379.

Andersson M, Blomstand F, Hanse E (2007) Astrocytes play a critical role in transient heterosynaptic depression in the rat hippocampal CA1 region. J Physiol 585:843–855.

Andrade-Talavera Y, Duque-Feria P, Paulsen O, Rodríguez-Moreno A (2016) Presynaptic spike timing-dependent long-term depression in the mouse hippocampus. Cereb Cortex 26:3637–3654.

Andrade-Talavera Y, Pérez-Rodríguez M, Prius-Mengual J, Rodríguez-Moreno A (2023) Neuronal and astrocyte determinants of critical periods of plasticity. Trends Neurosci 46:566–580.

Araque A, Carmignoto G, Haydon PG, Oliet SH, Robitaille R, Volterra A (2014) Gliotransmitters travel in time and space. Neuron 81:728–739.

Banerjee A, González-Rueda A, Sampaio-Baptista C, Paulsen O, Rodríguez-Moreno A (2014) Distinct mechanisms of spike timing-dependent LTD at vertical and horizontal inputs onto L2/3 pyramidal neurons in mouse barrel cortex. Physiol Rep 2:e00271.

Banerjee A, Meredith RM, Rodríguez-Moreno A, Mierau SB, Auberson YP, Paulsen O (2009) Double dissociation of spike timing-dependent potentiation and depression by subunit-preferring NMDA receptors antagonists in mouse barrel cortex. Cereb Cortex 19:2959–2969.

Beltrán-Castillo S, Olivares MJ, Contreras RA, Zúñiga G, Llona I, Von Bernhardi R, Eugenín JL (2017) D-serine released by astrocytes in brainstem regulates breathing response to CO2 levels. Nat Commun 8:838.

Bender VA, Bender KJ, Brasier DJ, Feldman DE (2006) Two coincidence detectors for spike timing-dependent plasticity in somatosensory cortex. J Neurosci 16:4166–4177.

Bi GQ, Poo MM (1998) Synaptic modifications in cultured hippocampal neurons: dependence on spike timing, synaptic strength, and postsynaptic cell type. J Neurosci 18:10464–10472.

Bidoret C, Ayon A, Barbour B, Casado M (2009) Presynaptic NR2A-containing NMDA receptors implement a high-pass filter synaptic plasticity rule. Proc Natl Acad Sci USA 106:14126–14131.

Bliss TV, Collingridge GL, Morris RG (2014) Synaptic plasticity in health and disease: introduction and overview. Philos Trans R Soc Lond B Biol Sci 369:20130129.

Brasier DJ, Feldman DE (2008) Synapse-specific expression of functional presynaptic NMDA receptors in rat somatosensory cortex. J Neurosci 28: 2199–2211.

Brigman JL, et al. (2010) Loss of Glu N2B-containing NMDA receptors in CA1 hippocampus and cortex impairs long-term depression, reduces dendritic spine density, and disrupts learning. J. Neurosci 30:4590–4600.

Brock JA, Thomazeau A, Watanabe A, Li SSY, Sjöström PJA (2020) A practical guide to using CV analysis for determining the locus of synaptic plasticity. Front. Synaptic Neurosci 12:11.

Brzosko Z, Mierau SB, Paulsen O (2019) Neuromodulation of spike-timing-dependent plasticity: past, present and future. Neuron 103:563–581.

Buonomano DV, Merzenich MM (1998) Cortical plasticity: from synapses to maps. Annu Rev Neurosci 31:25–46.

Bush D, Philippides A, Husbands P, O´Shea M (2010) Spike timing-dependent plasticity and the cognitive map. Front Comput Neurosci 4: 142.

Cajal SR (1894) The croonian lecture: la fine structure des centres nerveux. Proc R Soc Lond 55:444–468.

Campanac E, Debanne D (2008) Spike timing-dependent plasticity: a learning rule for dendritic integration in rat CA1 pyramidal neurons. J Physiol 586: 779–793.

Caporale N, Dan Y (2008) Spike timing-dependent plasticity: a Hebbian learning rule. Annu Rev Neurosci 31:25–46.

Chevaleyre V, Takahashi KA, Castillo PE (2006) Endocannabinoid-mediated synaptic plasticity in the CNS. Annu Rev Neurosci 29:37–76.

Dalton GL, Wu DC, Wang YT, Floresco SB, Phillips AG (2012) NMDA GluN2A and GluN2B receptors play separate roles in the induction of LTP and LTD in the amygdala and in the acquisition and extinction of conditioned fear. Neuropharmacology 62:797–806.

Dan Y, Poo MM (2006) Spike timing-dependent plasticity: from synapse to perception. Physiol Rev 86:1033–1048.

Debanne D, Gähwiler BH, Thompson SM (1994) Asynchronous pre- and postsynaptic activity induces associative long-term depression in area CA1 of the rat hippocampus in vitro. Proc Natl Acad Sci USA 91:1148–1152.

Debanne D, Gahwiler BH, Thompson SM (1998) Long-term synaptic plasticity between pairs of individual CA3 pyramidal cells in rat hippocampal slice cultures. J Physiol 507:237–247.

Duffy S, Labrie V, Roder JC (2008) D-serine augments NMDA-NR2B receptor-dependent hippocampal long-term depression and spatial reversal learning. Neuropsychopharmacology 33:1004–1018.

Durkee C, Kofuji P, Navarrete M, Araque A (2021) Astrocyte and neuron cooperation in long-term depression. Trends Neurosci 44:837–848.

Falcón-Moya R, et al. (2020) Astrocyte-mediated switch in spike timing-dependent plasticity during hippocampal development. Nat. Comm 11: 4388.

Feldman DE (2000) Timing-based LTP and LTD at vertical inputs to layer II/III pyramidal cells in rat barrel cortex. Neuron 27:45–56.

Feldman DE (2012) Spike timing-dependence of plasticity. Neuron 75:556–571.

Feldman DE, Brecht M (2005) Map plasticity in somatosensory cortex. Science 310:810–815.

Fischer G, Mutel V, Trube G, Malherbe P, Kew JN, Mohacsi E, Heitz MP, Kemp JA (1997) Ro 25-6981, a highly potent and selective blocker of *N*-methyl-d-aspartate receptors containing NR2B subunit. Characterization in vitro. J Pharmacol Exp Ther 283:1285–1292.

Froemke RC, et al. (2013) Long-term modification of cortical synapses improves sensory perception. Nat. Neurosci 16:79–88.

Froemke RC, Poo MM, Dan Y (2005) Spike timing-dependent synaptic plasticity depends on dendritic location. Nature 434:221–225.

Ghosh TK, Eis PS, Mullane JM, Ebert CL, Cl G (1988) Competitive, reversible, and potent antagonism of inositol 1,4,5-triphosphate-activated calcium release by heparin. J Biol Chem 263:11075–11079.

Han J, et al. (2012) Acute cannabinoids impair working memory through astroglial CB1 receptor modulation of hippocampal LTD. Cell 148: 1039–1050.

Haydon PG, Carmignoto G (2006) Astrocyte control of synaptic transmission and neurovascular coupling. Physiol Rev 86:1009–1031.

Henneberger C, Papouin T, Oliet SH, Rusakov DA (2010) Long-term potentiation depends on release of D-serine from astrocytes. Nature 463:232–236.

Koh W, et al. (2022) Astrocytes render memory flexible by releasing D-serine and regulating NMDAR tone in the hippocampus. Biol Psychiatry 91: 740–752.

Kutsuwada T, et al. (1996) Impairment of suckling response, trigeminal neuronal pattern formation, and hippocampal LTD in NMDA receptor epsilon 2 subunit mutant mice. Neuron 16:333–344.

Lalo U, Palygin O, Verkhratsky A, Grant SGN, Pankratov Y (2016) ATP from synaptic terminals and astrocytes regulate NMDA receptors and synaptic plasticity through PSD-95 multi-protein complex. Sci Reports 6:33609.

Le Meur K, Galante M, Angulo MC, Audinat E (2007) Tonic activation of NMDA receptors by ambient glutamate of non-synaptic origin in the rat hippocampus. J. Physiol 580:373–383.

Magee JC, Grienberger C (2020) Synaptic plasticity forms and functions. Ann Rev Neuroci 43:95–117.

Markram H, Lubke J, Frotscher M, Sakmann B (1997) Regulation of synaptic efficacy by coincidence of postsynaptic APs and EPSPs. Science 275:213–215.

Martínez-Gallego I, Cuaya HC, Rodríguez-Moreno A (2024) Astrocytes mediate two forms of spike timing-dependent depression at entorhinal cortex-hippocampal synapses. Elife 13:RP98031.

Martínez-Gallego I, Pérez-Rodríguez M, Coatl-Cuaya H, Flores G, Rodríguez-Moreno A (2022b) Adenosine and astrocytes determine the developmental dynamics of spike timing-dependent plasticity in the somatosensory cortex. J Neurosci 42:6038–6052.

Martínez-Gallego I, Rodríguez-Moreno A, Andrade-Talavera Y (2022a) Role of group I metabotropic glutamate receptors in spike timing-dependent plasticity. Int J Mol Sci 23:7807.

Mateos-Aparicio P, Rodríguez-Moreno A (2019) The impact of studying brain plasticity. Front Cell Neurosci 13:66.

Mateos-Aparicio P, Rodríguez-Moreno A (2020) Calcium dynamics and synaptic plasticity. Adv Exp Med Biol 1131:965–984.

Min R, Nevian T (2012) Astrocyte signaling controls spike timing-dependent depression at neocortical synapses. Nat Neurosci 15:746–753.

Monday HR, Younts TJ, Castillo PE (2018) Long-term plasticity of neurotransmitter release: emerging mechanisms and contributions to brain function and disease. Annu Rev Neurosci 41:299–322.

Mothet JP, Parent AT, Wolosker H, Brady RO Jr, Linden DJ, Ferris CD, Rogawski MA, Snyder SH (2000) D-Serine is an endogenous ligand for the glycine site of the N-methyl-D-aspartate receptor. Proc. Natl. Acad. Sci. USA 97:4926–4931.

Mothet JP, Pollegioni L, Ouanounou G, Martineau M, Fosier P, Baux G (2005) Glutamate receptors activation triggers a calcium and SNARE protein-dependent release of the gliotransmitter D-serine. Proc. Natl. Acad. Sci. USA 102:5606–5611.

Mulkey RM, Endo S, Shenolikar S, Malenka RC (1994) Involvement of calcineurin/inhibitor-1 phosphatase cascade in hippocampal long-term depression. Nature 369:486–488.
Nabavi S, Fox R, Proulx CD, Lin JY, Tsien RY, Malinow R (2014) Engineering a memory with LTD and LTP. Nature 511:348–352.
Nabavi S, Kessels HW, Alfonso S, Aow J, Fox R, Malinow R (2013) Metabotropic NMDA receptor function is required for NMDA receptor-dependent long-term depression. Proc Natl Acad Sci USA 110:4027–4032.
Navarrete M, et al. (2019) Astrocytic p38α MAPK drives NMDA receptor-dependent long-term depression and modulates long-term memory. Nat Commun 10:2968.
Navarrete M, Araque A (2008) Endocannabinoids mediate neuron-astrocyte communication. Neuron 57:883–893.
Navarrete M, Araque A (2010) Endocannabinoids potentiate synaptic transmission through stimulation of astrocytes. Neuron 68:113–126.
Nevian T, Sakmann B (2006) Spine Ca^{2+} signaling in spike-timing-dependent plasticity. J Neurosci 43:11001–11013.
Noriega-Prieto JA, Kofuji P, Araque A (2023) Endocannabinoid signaling in synaptic function. Glia 71:36–43.
Panatier A, Theodosis DT, Mothet JP, Touquet B, Pollegioni L, Poulain D, Oliet SHR (2006) Glia-derived D-serine controls NMDA receptor activity and memory. Cell 125:775–784.
Paoletti P, Bellone C, Zhou Q (2013) NMDA receptor subunit diversity: impact on receptor properties, synaptic plasticity and disease. Nat Rev Neurosci 14:383–400.
Papouin T, Dunphy JM, Tolman M, Dineley KT, Haydon PG (2017) Septal cholinergic neuromodulation tunes the astrocyte-dependent gating of hippocampal NMDAR to wakefulness. Neuron 94:840–854.
Papouin T, Ladépêche L, Ruel J, Sacchi S, Labasque M, Hanini M (2012) Synaptic and extrasynaptic NMDA receptors are gated by different endogenous coagonists. Cells 150:633–646.
Parpura V, Zorec R (2010) Gliotransmission: exocytotic release from astrocytes. Brain Res Rev 63:83–92.
Pascual O, Casper KB, Kubera C, Zhang J, Revilla-Sánchez R, Sul JY, Takano H, Moss SJ, McCarthy K, Haydon PG (2005) Astrocytic purinergic signalling coordinates synaptic networks. Science 310:113–116.
Pérez-Otaño I, Rodríguez-Moreno A (2019) Presynaptic NMDARs and astrocytes ally to control circuit-specific information flow. Proc Natl Acad Sci U S A 116:13166–13168.
Pérez-Rodríguez M, Arroyo-García LE, Prius-Mengual J, Andrade-Talavera Y, Armengol JA, Pérez-Villegas EM, Duque-Feria P, Flores G, Rodríguez-Moreno A (2019) Adenosine receptor-mediated developmental loss of spike timing-dependent depression in the hippocampus. Cereb Cortex 29: 3266–3281.
Pinto-Duarte A, Roberts AJ, Ouyang K, Sejnowski TJ (2019) Impairments in remote memory caused by the lack of type 2 IP3 receptors. Glia 7: 1976–1989.
Rasooli-Nejad S, Palygin O, Lalo U, Pankratov Y (2014) Cannabinoid receptors contribute to astroglial Ca^{2+} signalling and control of synaptic plasticity in the neocortex. Philos Trans R Soc Lond B Biol Sci 369:20140077.
Rodríguez-Moreno A, Banerjee A, Paulsen O (2010) Presynaptic NMDA receptors and spike timing-dependent depression at cortical synapses. Front Syn Neurosci 2:18.
Rodríguez-Moreno A, González-Rueda A, Banerjee A, Upton ML, Craig M, Paulsen O (2013) Presynaptic self-depression at developing neocortical synapses. Neuron 77:35–42.
Rodríguez-Moreno A, Kohl MM, Reeve J, Eaton TR, Collins HA, Anderson HL, Paulsen O (2011) Presynaptic induction and expression of timing-dependent long-term depression demonstrated by compartment specific photorelease of a use-dependent NMDA antagonist. J Neurosci 31: 8564–8569.
Rodríguez-Moreno A, Paulsen O (2008) Spike timing-dependent long-term depression requires presynaptic NMDA receptors. Nat Neurosci 11: 744–745.
Sardinha VM, et al. (2017) Astrocytic signaling supports hippocampal-prefrontal theta synchronization and cognitive function. Glia 65:1944–1960.
Sasaki T, Beppu K, Tanaka KF, Fukazawa Y, Shigemoto R, Matsui K (2012) Application of an optogenetic byway for perturbing neuronal activity via glial photostimulation. Proc Natl Acad Sci U S A 109:20720–20725.
Sjöström PJ, Turrigiano GG, Nelson SB (2003) Neocortical LTD via coincident activation of presynaptic NMDA and cannabinoid receptors. Neuron 39:641–654.
Torii N, Kamishita T, Otsu Y, Tsumoto T (1995) An inhibitor for calcineurin, FK506, blocks induction of long-term depression in rat visual cortex. Neurosci Lett 185:14.
Valtcheva S, Venance L (2016) Astrocytes gate Hebbian synaptic plasticity in the striatum. Nat Commun 7:13845.
Zhang Z, Gong N, Wang W, Xu L, Xu TL (2008) Bell-shaped D-serine actions on hippocampal long-term depression and spatial memory retrieval. Cereb Cortex 18:2391–2401.
Zhang JM, Wang HK, Ye CQ, Ge W, Chen Y, Jiang Z, Wu CP, Poo MM, Duan S (2003) ATP released by astrocytes mediates glutamatergic activity-dependent heterosynaptic suppression. Neuron 40:971–982.
Zhou Q, Sheng M (2013) NMDA receptors in nervous system diseases. Neuropharmacology 74:69–75.
Zhuang Z, Yang B, Theus MH, Sick JT, Bethea JR, Sick TJ, Liebl DJ (2010) Ephrinbs regulate D-serine synthesis and release in astrocytes. J Neurosci 30:16015–16024.